Fabrication of Nanofibrous PVA/Alginate-Sulfate Substrates for Growth Factor Delivery

Sajjad Mohammadi,[1,2] Seeram Ramakrishna,[3,6] Sophie Laurent,[4,7] Mohammad Ali Shokrgozar,[2] Dariush Semnani,[5] Davoud Sadeghi,[10] Shahin Bonakdar,[2] Mohsen Akbari[1,8,9]

[1]Laboratory for Innovations in Microengineering (LiME), Department of Mechanical Engineering, University of Victoria, Victoria, V8P 5C2, Canada

[2]National Cell Bank Department, Pasteur Institute of Iran, Tehran, 13164, Iran

[3]Center for Nanofibers and Nanotechnology, Department of Mechanical Engineering, National University of Singapore, Engineering Drive 3, 117576, Singapore

[4]NMR and Molecular Imaging Laboratory, Department of General, Organic and Biomedical Chemistry, University of Mons, 23 Place du Parc, B-7000, Mons, Belgium

[5]Department of Textile Engineering, Isfahan University of Technology, Isfahan, 84156-83111, Iran

[6]Institute of CNS Regeneration, Jinan University, Guangzhou, China

[7]Center for Microscopy and Molecular Imaging (CMMI), Rue Adrienne Bolland, 8, B-6041 Gosselies, Belgium

[8]Center for Biomedical Research, University of Victoria, Victoria, V8P 5C2, Canada

[9]Center for Advanced Materials and Related Technology (CAMTEC), University of Victoria, Victoria, V8P 5C2, Canada

[10]Department of Biomedical Engineering, Amirkabir University of Technology (Tehran Polytechnic), Tehran, Iran

Abstract: Providing affinity sites on alginate (ALG) matrix enables specific binding of growth factors to the polymer backbone and allows their release in a controlled fashion. In this study, we used a blend of alginate sulfate (ALG-S) and polyvinyl alcohol (PVA) to fabricate electrospun scaffolds capable of delivering a heparin-like growth factor, transforming growth factor-beta1 (TGF-β1). The alginate was sulfated with different degrees of sulfation (DS, from 0.8, 3.4 to 12.4%) by a simple process. The success of sulfation was determined by Fourier-transform infrared spectroscopy (FTIR), nuclear magnetic resonance spectroscopy (NMR), elemental analysis, ultraviolet (UV) spectroscopy and staining with dimethylmethylene blue. The physical-mechanical properties of nanofibrous mats were characterized by scanning electron microscopy (SEM), FTIR, energy-dispersive X-ray spectroscopy (EDX), tensile strength and mass loss analysis. Additionally, the release kinetics of transforming growth factor-β1 (TGF-β1) from PVA/ALG-S and PVA/ALG scaffolds were compared. The results showed that the binding and entrapment of TGF-β1 to the nanofibrous scaffolds are improved by the addition of sulfate group to alginate. In conclusion, our results support that nanofibrous scaffold based on PVA/ALG-S can deliver growth factors in tissue engineering application. © 2018 Wiley Periodicals, Inc. J Biomed Mater Res Part A: 00A: 000–000, 2018.

Key Words: alginate sulfate, polyvinyl alcohol, growth factor release, electrospun, tissue engineering, scaffolds

INTRODUCTION

Alginate (ALG) is an anionic polysaccharide derived from algae, which has found many applications in tissue engineering and drug delivery due to its biocompatibility, low toxicity, and mild gelation in the presence of calcium ions.[1–3] Alginate is an excellent scaffolding material as it can contain large amounts of water and can provide a three-dimensional (3D) environment similar to the extracellular matrix (ECM) for cells to grow and function in.[4–6] Hence, hydrogels of ALG have been extensively used for applications in skin, cartilage, bone, and cardiac tissue engineering.[2,7–11] Moreover, ALG is an attractive material for use in sustained delivery of bioactive molecules including drugs, proteins, and cells to wounds or damaged tissues.[2] Despite these excellent properties, pure ALG has several disadvantages including uncontrollable degradation, limited range of mechanical properties and lack of receptors for cellular binding.[6,12–14] The use of ALG for drug delivery applications has been limited by non-specific ionic

---

binding between the negatively charged ALG molecules and positively charged growth factors which lead to their uncontrolled release.[15–17] Therefore, providing affinity sites on the ALG matrix is crucial for specific binding of growth factors to the polymer backbone, which enables their release in a controlled fashion.

Sulfation state of the extracellular matrix (ECM) plays an important role in the regulation of growth factor signaling in native tissues. Sulfated matrixes made from synthetic or naturally-derived polymers have been recently used as a promising approach for stabilization and delivery of growth factors.[18] Recently, it has been shown that the sulfation of ALG can facilitate its reversible electrostatic interaction with heparin-binding proteins in a manner similar to heparin and heparan sulfate.[18–23] In an interesting study, Cohen *et al.* showed that the sulfation of ALG improved its binding with ten known heparin-binding proteins.[24] They achieved the sustained release of basic fibroblast growth factors (bFGF) by mixing ALG and ALG-S, and showed that the release profile was a function of the percentage of bFGF bound to the hydrogel. In another study, the same group used ALG-S for sustained release of transforming growth factor beta 1 (TGF-β1) to direct the differentiation of human mesenchymal stem cells (hMSCs) toward chondrocytes.[25] Ruvinov *et al.* used ALG-S to fabricate scaffolds for sequential delivery of three angiogenic factors of vascular endothelial growth factor (VEGF), platelet-derived growth factor-BB (PDGF-BB), and TGF-β1.[26] They showed that these growth factors bound to ALG-S with an affinity similar to heparin. In addition, delivering three factors enhanced the vascularization of tissues compared to scaffolds loaded with only bFGF. Re'em *et al.* developed a bilayer scaffold from ALG-S for simultaneous delivery of TGF-β1 and osteoinductive bone morphogenetic protein-4 (BMP-4) for cartilage and bone regeneration.[25] This method enabled them to control the migration of stem cells into subchondral defects and direct their differentiation into the appropriate cell lineage. Other growth factors including hepatocyte growth factor (HGF) and insulin-like growth factor-1 (IGF-1) were also delivered by ALG-S carriers for treatment of myocardial infarction.[27,28] Overall, ALG-S is a promising material for delivering growth factors for tissue engineering applications.

Nanofibrous scaffolds for drug delivery applications offer several advantages including the ability to fine-tune their mechanical and structural properties, their high surface to volume ratio, and having a microstructure that is similar to the ECM.[29–31] Nanofibrous scaffolds have highly porous structures with interconnected pores which can support infiltration, adhesion, proliferation, and migration of the cells within the scaffold as well as nutrients and waste exchange.[31] Pore size and distribution, which can be controlled in the electrospinning process, can affect cell infiltration and proliferation within the scaffold.[32–35] Also, interconnectivity of pores in the scaffold is more attainable in a nanofibrous matrix where the continuous form of electrospun nanofibers can generate inter-continuous pathways for delivering oxygen and nutrients to the cells.[32,36] Currently, electrospinning has proven to be an effective technique for fabrication of nanofibrous scaffolds from polymer solutions.[31,37,38] However, fabrication of electrospun scaffolds from naturally-derived hydrogels such as ALG/ALG-S remains a challenge. This is because ALG/ALG-S lacks chain entanglements owing to its rigid and extended chain conformation in aqueous solution. Also, gelation of the ALG/ALG-S solution begins at very low polymer concentrations.[39–42]

In this study, we report on the fabrication and characterization of nanofibrous ALG-S scaffolds using electrospinning for the first time. Electrospinnibility of ALG-S was improved by adding polyvinyl alcohol (PVA) to the alginate matrix. PVA is a water-soluble and biocompatible synthetic polymer which is chemically and thermally stable and has excellent wettability and biocompatibility.[43] Furthermore, fibrous structures made out of PVA have exhibited high mechanical strength and abrasion resistance. The aforementioned properties have made PVA an excellent polymer that can be blended with hydrogels for improving their mechanical properties and tuning their degradation kinetics.[43] Additionally, the hydroxyl groups of PVA molecules can increase the interfacial bonding in composites and thereby can promote the electrospinnibility of PVA electrospun fibers.[44,45] We optimized the electrospinning parameters for PVA/ALG and PVA/ALG-S and introduced a physical method for crosslinking the fabricated scaffolds. Morphology, degradation profile, tensile strength, cell attachment and viability on the fabricated scaffolds were evaluated *in vitro.* Moreover, the feasibility of loading TGF-β1, as a model of heparin-like growth factors, into the nanofibrous scaffolds was assessed and the effect of incorporating sulfate groups within the alginate matrix on the TGF-β1 release was evaluated. Our results suggest that the electrospun constructs made from PVA/ALG-S are promising scaffolds for local delivery of heparin-like proteins for tissue engineering applications.

RESULTS

To determine the effect of the degree of sulfation (DS) on the sulfate concentration within the gel, we added different concentration chlorosulfonic acid (ClSO$_3$H) to alginate hydrogels (Fig. 1A). Three batches of ALG-S were produced with "high" (12.4%), "medium" (3.4%), and "low" (0.8%) degrees of sulfation. Increasing the DS of the samples resulted in a change in their color from light yellow (ALG-S/Low) to dark brown (ALG-S/High) (Fig. 1B). Elemental analysis was used to quantify the extent of sulfation. The degree of sulfation was further quantified using the dimethyl methylene blue (DMMB) assay (Fig. S1). The color of the solutions changed with the degree of sulfation of the ALG-S samples. The measured concentrations of sulfate in low, medium, and high DS samples were 7.7, 14.1, and 55.1 µg/mL, respectively (Fig. 1C). Ultraviolet (UV) absorption spectra of the powders prepared from ALG-S with different degrees of sulfation (Fig. S2) showed higher absorption of UV in the range of 260–280 nm for samples with high DS. We used high DS in the rest of the experiments. Nuclear magnetic resonance
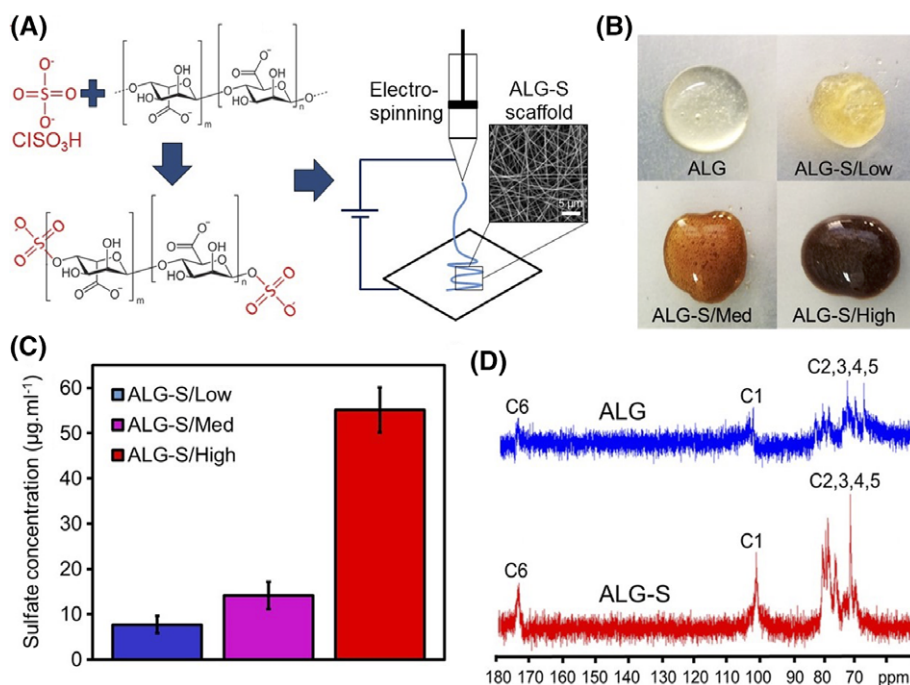
FIGURE 1. Fabrication and characterization of electrospun PVA/ALG-S scaffolds. (A) Schematic of the process of synthesizing ALG-S and electrospinning of the scaffold. ALG-S was prepared at different sulfation degrees of low (0.8%), medium (3.4%), and high (12.4%). The inset shows a scanning electron microscopy (SEM) of a typical electrospun scaffold. (B) Optical images of ALG with different sulfation degrees. Increasing the sulfation degree resulted in darker solutions. (C) Concentration of sulfate in ALG-S at different sulfation degrees of low, medium, and high. (D) NMR spectra of ALG and ALG-S. The chemical shifts of C1 and C6 of the guluronic acid can be observed at ~100 and 177 ppm, respectively, which reveals that the sulfation reaction of ALG do not include C1or C6 substitution.

(13C NMR) data demonstrated the chemical shifts of C1 and C6 of the guluronic acid at ~100 and 177 ppm, respectively; this revealed that the sulfation reaction of ALG did not include C1 or C6 substitution (Fig. 1D). Furthermore, the chemical shifts of C2, C3, C4, and C5 were found to be between 60–80 ppm, which is in good agreement with previous studies.[21,32] After sulfation, the chemical shifts of ALG became more complicated and the carbons C2 and C3 moved to lower field positions while C4 and C5 shifted to a higher field position.

Fourier transform infrared (FTIR) spectra of ALG and ALG-S is shown in Figure 2A. For the sulfated alginate, peaks characteristic to S=O stretching were confirmed with FTIR spectra at 1250 cm^{-1}. A minor peak was also detected at 873 cm^{-1}, which represented a symmetrical C–O–S vibration associated to a C–O–SO$_3$ group. Figure 2B shows the FTIR
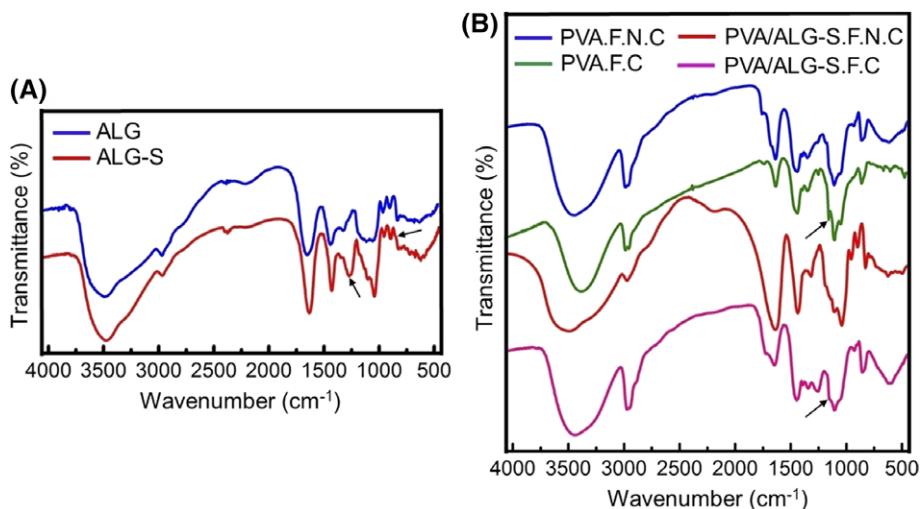

FIGURE 2. FTIR spectra of (A) alginate (ALG), alginate sulfate (ALG-S) and (B) non-crosslinked PVA nanofibers (PVA.F.N.C), crosslinked PVA nanofibers (PVA.F.C), non-crosslinked PVA/ALG-S nanofibers (PVA/ALG-S.F.N.C), crosslinked PVA/ALG-S nanofibers (PVA/ALG-S.F.C). All ALG-S samples are high DS.
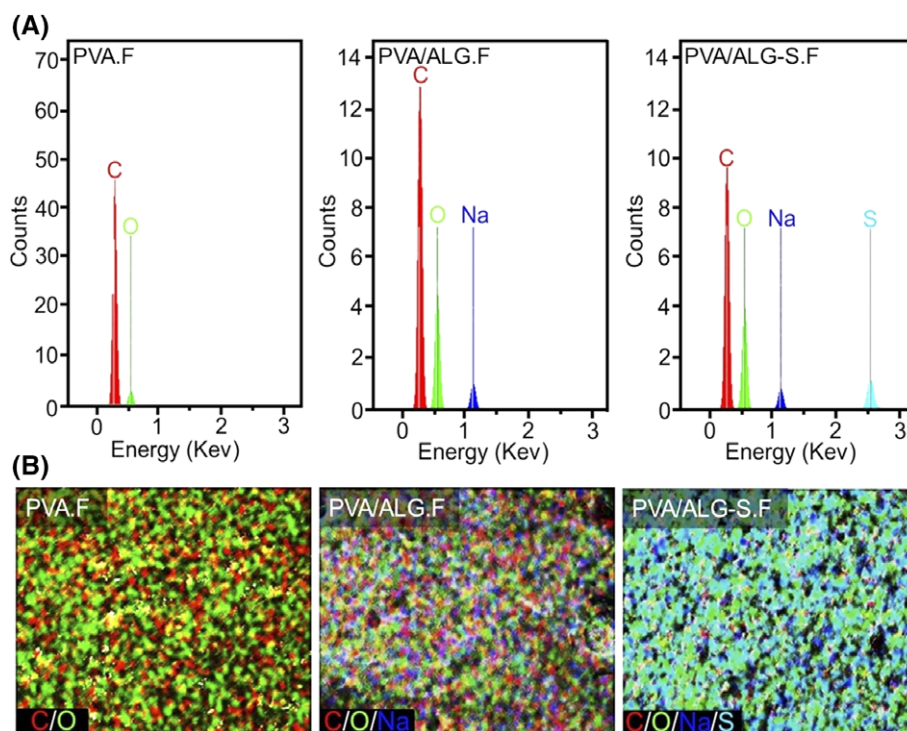
FIGURE 3. EDX of the electrospun scaffolds. (A) The point scanning of the scaffolds surfaces made from PVA, PVA/ALG, and PVA/ALG-S. (B) The map scanning of the scaffolds surfaces made from PVA, PVA/ALG, and PVA/ALG-S showing carbon (red), oxygen (green), sodium (blue), and sulfate (cyan). All ALG-S samples are high DS.

spectra of non-crosslinked and crosslinked polymers. The characteristic peak in PVA spectra is at 3337 cm^{-1}, which represents the bending vibration of hydroxyl groups. Also, the 2941 cm^{-1} peak represents CH2, the 1709 cm^{-1} shows the C=O bending vibration, the 1092 cm^{-1} stands for the C–O group and 850 cm^{-1} is attributed to the C–C group stretching vibration.[46] . The peaks at 3446 cm^{-1}, 624 cm^{-1} and 1420 cm^{-1} correspond to hydrogen-bonded OH groups, asymmetric COO- and symmetric COO- stretching vibrations in ALG, respectively.[47,48] The spectra showed two absorption peaks, one at ~1050 cm^{-1} relating to S=O stretching vibration and another one at ~720 cm^{-1} corresponding to S-O-C vibration. We also noticed two other absorption peaks, one at ~1050 cm^{-1} relating to the S=O stretching vibration and the other at ~720 cm^{-1} corresponding to the S-O-C vibration. The peak at 1141 cm^{-1} is caused by the ether group (C-O-C) in all crosslinked nanofibrous scaffolds.[48].

Figure 3 shows the Energy-dispersive X-ray spectroscopy (EDX) results of scaffolds made from PVA, PVA/ALG, and PVA/ALG-S. Point scanning on the surfaces of the scaffolds revealed the presence of O and C elements in the PVA

TABLE I. Stoichiometric Ratio of PVA/ALG composites

Sample	Element			
	Carbon	Oxygen	Sodium	Sulfur
PVA	78.35	21.65	0	0
PVA/ALG	52.50	44.84	2.66	0
PVA/ALG-S	49.49	45.51	2.09	2.91

scaffolds, and O, C and Na elements in PVA/ALG scaffolds. An additional S element was detected in PVA/ALG-S due to the sulfation of ALG (Fig. 3A). Weight percent of each element was given in Table I A map scanning showed the homogeneous distribution of each element on the scaffold surfaces (Fig. 3B).

We characterized the mechanical properties of the fabricated electrospun sheets as these are crucial parameters for design and optimization of engineered tissue substitutes. Tensile stress–strain curves revealed the effect of the cross-linking process on the tensile strength of the scaffolds (Fig. 4A). The effect of sulfation on the ultimate tensile strength of crosslinked and non-crosslinked scaffolds is shown in Figure S3B. Our results indicated that the cross-linking process significantly increased the elongation and ultimate strength of the scaffolds. However, sulfation of ALG had insignificant influence on the mechanical properties of the scaffolds.

The degradation profile of the fibrous structures made from PVA, PVA/ALG, and PVA/ALG-S is shown in Figure S3A. All samples were thermally crosslinked. Scaffolds that were made from PVA presented a faster degradation rate compared to those that were made from PVA/ALG blends. The faster degradation rate was attributed to the formation of hydrogen bonding between the carboxylate group of ALG and the hydroxyl group of PVA.[49,50] No significant change in the degradation rate of sulfated and non-sulfated was observed. We assessed the growth factor binding and entrapment of the nanofibrous scaffolds that were made from PVA/ALG and PVA/ALG-S (Fig. S3). Before the release
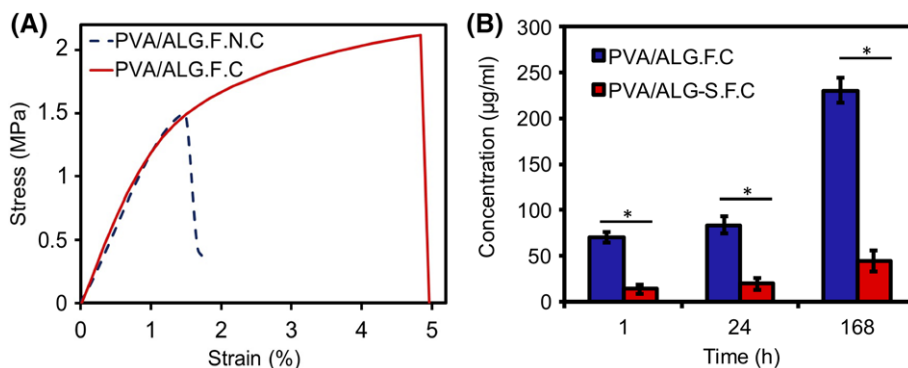
FIGURE 4. Physical and release properties of the PVA, PVA/ALG and PVA/ALG-S nanofibrous scaffolds. (A) Representative uniaxial stress–strain curve of crosslinked and non-crosslinked ALG fibrous scaffolds. (B) Released TGF-β1from nanofibrous scaffolds made from alginate sulfate and bare alginate after 7 days. Error bars represent SD of triplicates (* < 0.05).

studies, TGF-β1 was physically adsorbed in the scaffolds for 24 h and washed with phosphate buffer solution (PBS, pH 7.4 at 25 °C) to remove the protein residues on the surface of the scaffolds. The cumulative percentage release of TGF-β1 from scaffolds was then measured in after 1, 24, and 168 h using enzyme linked immunosorbent assay (ELISA). The release of TGF-β1 from PVA/ALG scaffolds was faster than PVA/ALG-S scaffolds due to the electrostatic interaction of TGF-β1 with ALG-S (Fig. 4B).

The effect of blending PVA with ALG on the morphology of the nanofibers was assessed using SEM (Fig. 5A). Heterogeneous fibers containing many beads were observed in the PVA sample. In contrast, the addition of ALG and ALG-S to PVA led to the formation of uniform nanofibers without any beads. SEM images of the crosslinked scaffolds demonstrated that the morphology of the nanofibers was similar to that of non-crosslinked scaffolds. Cell attachment to the scaffolds was evaluated by seeding human derived mesenchymal stem cells (hMSCs) on the electrospun scaffolds. Scanning electron microscopy images of the cells were taken after 24 h of seeding (Fig. 5B). Due to the faster degradation rate of the PVA scaffolds, larger pore sizes were observed in these scaffolds compared to those that were blended with ALG. Moreover, cells attached better to the PVA/ALG scaffolds as they maintained their integrity due to the slower degradation rate. This was further confirmed by staining the F-actin filaments of the cells after four days in culture (Fig. S4A). Figure S4B displays the results of the cell viability of HMSCs was used to evaluate the cytotoxicity of the nanofibrous mats in comparison with the control. All the samples (PVA, PVA/ALG, and PVA/ALG-S nanofibrous scaffold) showed cell viability greater than 90% in accordance to the control extraction media.

We measured the diameter of the fibers in the fabricated nanofibrous scaffolds by analyzing the SEM images of each scaffold. The diameters of randomly-selected fibers (n = 100) were measured when the scaffolds were not crosslinked, crosslinked, and exposed to the cells. Figure S5A shows the size distribution for non-crosslinked PVA scaffolds. Fiber diameters were in the range of 97 nm to 2.8 m with the average diameter of 391 ± 400 nm. Interestingly,

blending PVA with alginate significantly affected the uniformity of the fiber diameters in the nanofibrous scaffolds. For example, the size distribution of the fibers made from PVA/ALG was in the range of 137 to 385 nm with the average diameter of 232 ± 52 nm (Fig. S5B). However, sulfation of alginate did not have a significant effect on the size distribution and average diameter of the nanofibers (Fig. S5C). The range of fiber diameter for scaffolds made from PVA/ALG-S was from 164 to 470 nm, and the average fiber diameter was 273 ± 58 nm. We also investigated the effect of crosslinking on the size distribution of nanofibers. Overall, the size of the nanofibers slightly increased after the crosslinking process (Fig. S5D-E). The average fiber diameters were 637 ± 532 nm, 275 ± 50 nm, and 239 ± 47 nm for PVA, PVA/ALG, and PVA/ALG-S, respectively. When cells were seeded on the scaffolds, the diameter of the fibers increased considerably due to swelling (Fig. S5D-E). The increase in the fiber diameter was more pronounced in structures that were made from PVA alone. The average fiber diameters for PVA, PVA/ALG, and PVA/ALG-S were 2.89 ± 2.0 nm, 319 ± 81 nm, and 365 ± 91 nm, respectively.

DISCUSSION

Alginate is a biocompatible hydrogel with many applications in wound healing, drug delivery, and tissue engineering. Alginate gels have been widely used for delivering low molecular weight drugs, in particular when a primary or secondary bond between the drug and the ALG is formed to modulate the release kinetics of the drug. Due to the hydrophilicity and relatively large pore sizes of ALG gels (5 nm).[51], proteins such as VEGF, bFGF, and TGF-β1 can be rapidly released from the ALG microcarriers. However, the kinetics of release cannot be controlled accurately because of the uncontrolled degradation rate of ALG *in vivo.* In this study, we sulfated ALG to provide affinity sites on the hydrogel matrix for specific binding of growth factors to the polymer backbone. Alginate was sulfated using two protocols. The first protocol was followed as described by Fan *et al.*[52] However, elemental analysis indicated that DS of 0.9% was obtained using this protocol. In order to enhance growth factor adsorption,
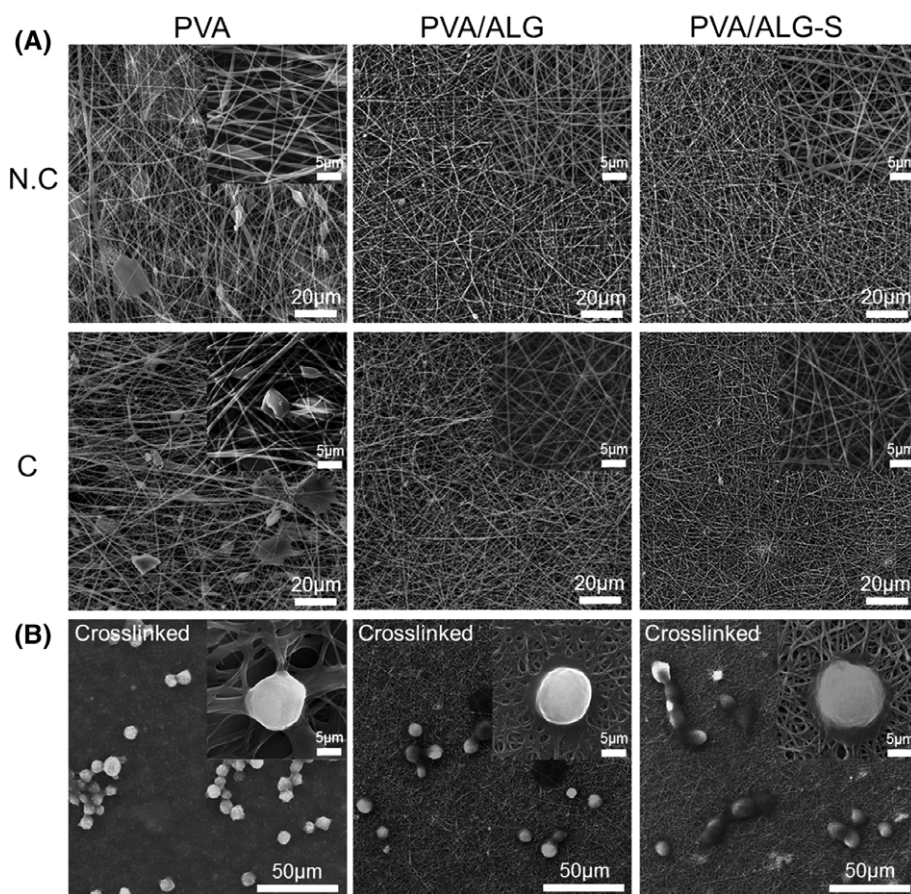
FIGURE 5. (A) SEM images of the scaffolds made from crosslinked (C) and non-crosslinked (N.C) PVA, PVA/ALG, and PVA, ALG-S scaffolds. (B) Attachment of cells to the scaffolds.

higher DS is required. Thus, the protocol described by Ronghua *et al*. was followed to obtain a higher DS of ALG.[53] This method presents some advantages over protocols described in literature.[24,52] including defined DS, high efficiency, simplicity, low cost, etc.[54] Elemental analysis demonstrated that DS of 12.4% was obtained via this process while other applied sulfation protocols resulted in lower DS. Ronghua *et al*. also reported similar results.[53]

The process of ALG sulfation was characterized by ^{13}C NMR and FTIR. Lack of chemical shift of C1 and C6 in ^{13}C NMR spectra means that sulfate groups were not added to those carbons and were mainly added to the OH groups (either one of the C2 or C3 or both) of uronic acid. The shift of the carbons C2 and C3 to lower field position was due to the direct attachment of electronegative sulfate ester groups, while the shift of C4 and C5 to higher field positions was a result of indirect attachment to sulfate ester groups, as shown previously by others.[24,52,53] The sulfation of uronic acid in ALG was also indicated by the absorption peaks in FTIR spectra of S=O and S-O-C vibration, in good agreement with previous studies.[24,52,53] Furthermore, crosslinking of the mixed scaffolds was identified by a peak of ether group (C-O-C) which was obtained from the crosslinking of PVA.[48]

Evidence showed the poor electrospinnability of PVA with the molecular weight of 144,000 g.mol^{−1}. Many beads

were formed during the process, mainly due to the instability of the solution. However, when PVA was blended with ALG or ALG-S, more uniform nanofibers were formed. This behaviour is related to the higher viscosity of the PVA/ALG blend compared to the pure PVA.[49] According to the SEM images, it can be concluded that electrospinnability of both PVA and ALG (or ALG-S) have been promoted by blending. Also, blending PVA/ALG and PVA/ALG-S nanofibrous scaffolds resulted in better crosslinking and cell attachment compared to the PVA nanofiber counterpart.

Researchers have used many chemical and physical methods to crosslink PVA based nanofibrous scaffolds in order to reduce their water solubility.[55-57] Since the chemical methods yield toxic products.[58,59], in this study, PVA/ALG and PVA/ALG-S nanofibrous scaffolds were crosslinked by a physical method (heating at 150 °C).

Polyvinyl alcohol with molecular weight of 144,000 g. mol^{−1} was used to obtain higher tensile strength.[60,61] A decrease in the tensile strength of PVA with addition of ALG and ALG-S as a result of the indisposition of homogeneity of the polymeric substrate has been reported previously.[62] Crosslinking increases elongation at the break of the scaffold. In addition, physically crosslinking enhances the tensile strength of all scaffolds.[63,64] Moreover, a higher degree of crosslinking of the scaffolds containing ALG and ALG-S

lowered the mass loss in comparison with physically cross-linked PVA scaffolds.[65] The ALG-S nanofibrous scaffolds showed a favorable entrapment of the loaded TGF-β1 due to the higher affinity of the ALG-S over ALG for binding to TGF-β1.

Figure 4B displays the results for growth factor delivery and shows the slow release of TGF-β1 from ALG-S fibers in comparison with ALG. In the body, growth factors are attached to heparin and the presence of sulfate groups on alginate structure is similar to heparin structure.[16,17,54,66] It has been shown previously that most heparin-binding proteins do not bind to bare alginate, however, they strongly bind to sulfated alginate via electrostatic interactions.[24] Alginate has a nanoporous matrix with the pore size in the order of a few nanometers, leading to rapid diffusion of proteins through the gel.[67] However, heparin-binding growth factors such as vascular endothelial growth factor (VEGF), TGF-β1, and basic fibroblast growth factor (bFGF) exhibit reversible binding to sulfated alginate, enabling sustained release due to the hydrolysis of the gel.[15,24–27,66] The release kinetics can be manipulated by changing the degradation rate of the gels by the use of partially oxidized alginate.[67] Our results demonstrated that the sulfation of alginate matrix promoted protein attachment to the alginate matrix, thereby significantly slower release rates were achieved compared to bare alginate.

The morphology and fiber diameter plays an important role on the interaction of the scaffolds and the cells and the release kinetic of the drugs. We examined the effect of blending alginate and PVA on the microstructure of the electrospun scaffolds and size distribution of the nanofibers. Becuase of the poor electrospinnibility of PVA, the pore size and size distribution of the fibers were not uniform in the scaffolds that were made from PVA alone. However, blending alginate with PVA improved the ability to electrosping these materials as demonstrated by the uniform size distribution of nanofibers shown in Figure S5D-F. Overall, the crosslinking process did not influence the size distribution of the scaffolds. However, due to the expansion of the polymers during the thermal treatment, the average diameter of the nanofibers was slightly higher than the non-crosslinked scaffolds. Moreover, when cells were seeded on the scaffolds, the scaffolds that were made from PVA/ALG and PVA/ALG-S showed better integrity.

CONCLUSIONS

This study reports the first electrospun scaffold made from sulfated ALG. The sulfation of ALG at different degrees was successfully performed and characterized. To enhance the manufacturability of the sulfated ALG, it was blended with PVA and thermally crosslinked to form mechanically stable scaffolds. The mechanical properties of the crosslinked blend were significantly improved compared to the non-crosslinked mixture. We also observed a slightly slower degradation rate for the PVA/ALG blend compared to pure PVA. The release profile of TGF-β1 from scaffolds made from sulfated ALG was more sustained compared to the non-sulfated

scaffolds; this shows the potential of such constructs for growth factor delivery in tissue engineering. Moreover, biocompatibility assessments revealed a favorable and supportive cellular environment for hMSCs *in vitro*. All of the findings showed that blending ALG-S with PVA could overcome the disadvantages of both polymers and result in a suitable scaffold with tremendous potential for application in tissue engineering.

EXPERIMENTAL SECTION
Materials

Alginate (ALG,100–300 cP, 2%(25 °C)), chlorosulfonic acid (ClSO$_3$H, 99%), chondroitin sulfate (CS), formamide (1.128–1.132 g.mL^{-1}), tritonX-100, paraformaldehyde, Hoechst reactives, DMMB and phalloidin were purchased from Sigma Aldrich (USA). Polyvinyl alcohol (PVA, Mn = 144,000 g.mol^{-1} and 98% hydrolysis), acetone, glutaraldehyde (GTA) (50%)), were purchased from Merck company (Germany). Dulbecco modified Eagle medium (DMEM) and penicillin–streptomycin were purchased from Gibco-BRL, (Life Technologies, Rockville, MD, USA). Fetal bovine serum (FBS) was purchased from NanoBioArray, Iran.

Sulfating of ALG

In order to sulfate the ALG, Formamide/ClSO3H solutions were prepared with three different ratios (80:1, 80:5 and 80:20), and ALG (10 g) was added to each solution. The mixture was then preserved at 60 °C for 4 h to obtain a brown paste. 200 mL of acetone was added to precipitate the solution. The precipitate was redissolved in distilled water while the pH of the obtained solution was adjusted to 11 and dialyzed for 72 h.[53]

Preparation of nanofibrous scaffolds

A solution containing 5 wt% of PVA and 1 wt% of ALG and ALG-S12.4 were electrospun. Also, a PVA solution (10 wt%) was electrospun as control. The polymer solution was prepared by dissolving PVA in deionized water for 2 h and under continuous stirring at 90 °C. After that, ALG and ALG-S powders were added to the cooled solution at 25 °C separately and the stirring was continued for 3 h to obtain homogeneous polymer blend solutions. To produce electrospun scaffolds, syringes fitted with 21-G needles were utilized. The optimized parameters were 30 kV and 12 cm for distance between the needle tip and the collector and 18 mL.h^{-1} for flow rate.

Crosslinking of nanofibers

The nanofibrous scaffolds were physically crosslinked by heating at 150 °C for 24 h, and then cooled to 25 °C.

Elemental analysis

Sulfation degree (DS) of the ALG-S samples was determined by high-resolution inductively coupled plasma mass spectrometry (HR-ICP-MS). Specimens were prepared via dissolving 5 mg of ALG-S in 0.1 M HNO$_3$ (45 mL). The measured sulfur content in ALG-S powder was used to determine the DS. The DS is defined as the average number of sulfate

groups per ALG monomer.[53] using Equation 1 where x represents the DS.[54].

$$\text{Total monomer mass} = C_6H_5O_6 + (x+1)\,Na^+ + x\,SO_3^- + H_2O \quad (1)$$

It was expected in Equation 1 that almost 10% water was accompanying the ALG.

Ultraviolet (UV) spectroscopy: UV absorption of the stock solutions (16 µg.ml^{-1}) of different ALG-S powders with determined DS (0%, 0.8%, 3.4% and 12.4%, which was proven by elemental analyses) was analyzed by ePoch spectrophotometer (Biotech instruments, USA). CS was used as control and data was recorded over the wavelength range of 200–800 nm.

Dimethyl methylene blue (DMMB) staining: DMMB binds to sulfated glycosaminoglycans and changes from blue to purple.[68,69] We proposed that DS can be easily determined by DMMB staining protocol. This assay was performed by an ELISA reader (statfax2100, USA) in a 96 well plate with CS as control at wavelength of 545 nm. Different ALG-S samples with various DS (0%, 0.8%, 3.4% and 12.4%) were used. The stock solutions with different concentrations (0, 0.53, 1.1, 2.15, 5.33, 10.1 and 16 µg.ml^{-1}) and CS in buffer (0.05 M of sodium acetate, 0.05% of tween 20, at pH 6.8) were prepared. DMMB (at the concentration of 16 µg.ml^{-1}) was dissolved in 0.03 M of sodium formate and 0.2% v/v of formic acid. 75 µL of each stock solution, 25 µL of guanidine hydrochloride (2.88 M in buffer) and 200 µL of DMMB solution were added to each well.

Nuclear magnetic resonance (NMR) spectroscopy

Both ALG and ALG-S were dissolved in deionized water. ^{13}C NMR experiments were recorded at 25 °C on a Bruker Avance 400 MHz spectrometer (Bruker BioSpin AG, Germany) equipped with a 5 mm cryogenic CP-TCI z-gradient probe. Tetramethylsilane (TMS) was used as the internal standard. The ^{13}C NMR data were analyzed with TopSpin 3.0 software (Bruker BioSpin AG, Germany).

Fourier transform infrared (FTIR) spectroscopy: FTIR spectroscopy (PerkinElmer, USA) was performed to identify the chemical structure of the samples. The specimens were mixed with KBr to make sample pellets prior to examination. The spectra were scanned between 400 and 4000 cm^{-1}.

Scanning electron microscopy (SEM)

A field-emission scanning electron microscopy (FE-SEM; Philips XL30-Holland) equipped with energy dispersive X-ray spectroscopy (EDX; Link WDX-3PC-USA) was used to investigate the morphology of the nanofibrous scaffolds. Surfaces of the nanofibrous scaffolds were sputter-coated with gold (Au) prior to examination. To evaluate the DS of sulfated ALG, point scanning and map scanning were performed by an EDX.

Mechanical properties

Tensile strength of nanofibrous scaffolds were analyzed as described previously.[5] using a uniaxial tensile machine (Instron TM - SM, England**)** with a load cell of 10 N capacity.

The scaffolds were cut into rectangular strips of 1 × 2 cm^2 dimension and fixed vertically on the gripping unit of the tensile tester. Specimens were drawn at a crosshead speed of 10 mm.min^{-1} and data were recorded every 50 ms.

In vitro mass loss

The nanofibrous scaffolds were cut into square shapes and weighed. The scaffold were soaked in phosphate-buffered saline (PBS at pH = 7.4) and incubated at 37 °C. At specified times specimens were taken out from the incubator, washed with dionized water and vacuum-dried at 40 °C for 48 h.[70] Mass loss of the scaffold was calculated over a 2-month time period using Equation 2.

$$\text{Mass loss}\,(\%) = ((Wo - Wt)/Wo) \times 100 \quad (2)$$

Where Wo and Wt are the dry mass of the specimens before and after the degradation, respectively.

Cell culture

Human mesenchymal stem cells (hMSCs) isolated from abdominal adipose tissue were supplied from National Cell Bank of Iran, Pasteur Institute of Iran, Tehran, Iran. The medium consisted of DMEM-ham's F12 supplemented with 10% fetal bovine serum and 100 µg.ml^{-1} penicillin–streptomycin.

Cell attachment

In order to investigate the cell attachment by SEM, 5 × 10^5 cells obtained from third subculture of HMSCs were seeded on each specimen and incubated for 4 h. After removal of the culture medium, the specimens were rinsed in PBS twice and fixed by glutaraldehyde 4% solution. The samples were then dehydrated in graded alcohols and sputter coated by gold.

Cell actin staining

The cell actin staining was performed according to protocol described in literature.[71,72] Briefly, the cells were fixed by paraformaldehyde (4% in PBS) and permeabilized using tritonX-100 (0.1% in PBS). Afterwards, the cells were incubated for 45 min by a 0.2 µg.ml^{-1} solution of phalloidin in PBS to stain the actin filaments. Finally, cell nuclei were stained by a solution of Hoechst (1.5 µg.ml^{-1} in PBS) for 5 min and electrospun nanofibers were observed by a fluorescence microscope (Hund, Wilovert 30, Germany).

In vitro cytotoxicity by MTT assay

To determine the toxicity of the samples, HMSCs used for MTT assay according to ISO 10993-5. The nanofibrous scaffolds were cut into rectangular shapes of 2 cm × 1 cm. Each sample was immersed in 1 mL of serum-free culture medium DMEM-ham's F12 for 7 days at 37 °C. The serum-free culture medium without nanofibers was also incubated at 37 °C in the mentioned times and used as control. Briefly, cells were plated into a 96-well microtiter plate at 1 × 10^4 cells/well and 100 mL of DMEM-ham's F12 supplemented by 10% FBS was added to each well and incubated for 24 h

at 37 °C. After 24 h incubation, the culture medium of each well removed and replaced with 100 mL MTT (Sigma, USA) solution (0.5 mg ml^{-1} in PBS) was added to each well and incubated for 4 h at 37 °C. Finally, the MTT solution was removed and 100 mL isopropanol (Sigma, USA) was added to per well. The plates were then incubated at 37 °C for 15 min prior to absorbance measurements. The optical density (OD) was recorded on Absorbance at 570 nm was read on a multiwell microplate reader (ICN, Switzerland) at 545 nm and normalized to the control OD. The cell toxicity can be obtained according to the following Equation 3.

$$Toxicity\% = 1 - \frac{mean\ of\ OD\ sample}{mean\ of\ OD\ control} \times 100 \qquad (3)$$

TGF-β1 release study

A TGF-β1 Enzyme-Linked Immuno-sorbent Assay (ELISA, Biolegend, USA) kit was used to quantify the release rate of growth factor based on supplier instructions. 250 ng.ml^{-1} TGF-β1 (Biolegend) was added to each sample (PVA/ALG and PVA/ALG-S). After 24 h, the remaining growth factor solutions were discarded and fresh deionized water added. The amount of released TGF-β1 was detected by ELISA reader (statfax2100, USA) at specified intervals (1 h, 24 h and 128 h).

Statistical analysis

Statistical calculations were performed on GraphPad Prism 6, ANOVA test was used to analyze the data. $p < 0.05$ was considered statistically significant.

ACKNOWLEDGMENT

REFERENCES

1. Pawar SN, Edgar KJ. Chemical modification of alginates in organic solvent systems. Biomacromolecules 2011;12(11):4095–4103.
2. Mirani B et al. *An advanced multifunctional hydrogel-based dressing for wound monitoring and drug delivery*. Advanced healthcare materials 2017;6(19):1700718.
3. Santagapita PR, Mazzobre MF, Buera MP. Formulation and drying of alginate beads for controlled release and stabilization of invertase. Biomacromolecules 2011;12(9):3147–3155.
4. Tamayol A, Najafabadi AH, Aliakbarian B, Arab-Tehrany E, Akbari M, Annabi N, Juncker D, Khademhosseini A. Hydrogel templates for rapid manufacturing of bioactive fibers and 3D constructs. Adv Healthc Mater 2015;4(14):2146–2153.
5. Akbari M, Tamayol A, Laforte V, Annabi N, Najafabadi AH, Khademhosseini A, Juncker D. Composite living fibers for creating tissue constructs using textile techniques. Adv Funct Mater 2014; 24(26):4060–4067.
6. Ghorbanian S, Qasaimeh MA, Akbari M, Tamayol A, Juncker D. Microfluidic direct writer with integrated declogging mechanism for fabricating cell-laden hydrogel constructs. Biomed Microdevices 2014;16(3):387–395.
7. Madl CM, Mehta M, Duda GN, Heilshorn SC, Mooney DJ. Presentation of BMP-2 mimicking peptides in 3D hydrogels directs cell fate commitment in osteoblasts and mesenchymal stem cells. Biomacromolecules 2014;15(2):445–455.
8. Venkatesan J, Bhatnagar I, Manivasagan P, Kang KH, Kim SK. Alginate composites for bone tissue engineering: A review. Int J Biol Macromol 2015;72:269–281.
9. Desai RM, Koshy ST, Hilderbrand SA, Mooney DJ, Joshi NS. Versatile click alginate hydrogels crosslinked via tetrazine–norbornene chemistry. Biomaterials 2015;50:30–37.
10. Samorezov JE, Alsberg E. Spatial regulation of controlled bioactive factor delivery for bone tissue engineering. Adv Drug Deliv Rev 2015;84:45–67.
11. Pedde RD, Mirani B, Navaei A, Styan T, Wong S, Mehrali M, Thakur A, Mohtaram NK, Bayati A, Dolatshahi-Pirouz A, Nikkhah M, Willerth SM, Akbari M. Emerging Biofabrication Strategies for Engineering Complex Tissue Constructs. Adv Mater 2017;29:160606.
12. Briquez PS, Clegg LE, Martino MM, Gabhann FM, Hubbell JA. Design principles for therapeutic angiogenic materials. Nature Reviews Materials 2016;1:15006.
13. Rufaihah AJ, Seliktar D. Hydrogels for therapeutic cardiovascular angiogenesis. Adv Drug Deliv Rev 2016;96:31–39.
14. Peppas NA, Hilt JZ, Khademhosseini A, Langer R. Hydrogels in biology and medicine: from molecular principles to bionanotechnology. Adv Mater 2006;18(11):1345–1360.
15. Ruvinov E, Cohen S. Alginate biomaterial for the treatment of myocardial infarction: Progress, translational strategies, and clinical outlook: From ocean algae to patient bedside. Adv Drug Deliv Rev 2015;96:54–76.
16. Dvir T, Timko BP, Kohane DS, Langer R. Nanotechnological strategies for engineering complex tissues. Nat Nanotechnol 2011;6(1): 13–22.
17. Jeon O, Wolfson DW, Alsberg E. In-Situ Formation of Growth-Factor-Loaded Coacervate Microparticle-Embedded Hydrogels for Directing Encapsulated Stem Cell Fate. Adv Mater 2015; 27(13):2216–2223.
18. Öztürk E, Arlov Ø, Aksel S, Li L, Ornitz DM, Skjåk-Braek G, Zenobi-Wong M. Sulfated Hydrogel Matrices Direct Mitogenicity and Maintenance of Chondrocyte Phenotype through Activation of FGF Signaling. Adv Funct Mater 2016;26(21):3649–3662.
19. Ren X, Feng Y, Guo J, Wang H, Li Q, Yang J, Hao X, Lv J, Ma N, Li W. Surface modification and endothelialization of biomaterials as potential scaffolds for vascular tissue engineering applications. Chem Soc Rev 2015;44(15):5680–5742.
20. Babavalian H, Latifi AM, Shokrgozar MA, Bonakdar S, Mohammadi S, Moosazadeh Moghaddam M. Analysis of healing effect of alginate sulfate hydrogel dressing containing antimicrobial peptide on wound infection caused by methicillin-resistant *Staphylococcus aureus*. Jundishapur journal of microbiology 2015;8(9):e28320.
21. Vulic K, Shoichet MS. Affinity-based drug delivery systems for tissue repair and regeneration. Biomacromolecules 2014;15(11): 3867–3880.
22. Arlov Ø, Aachmann FL, Feyzi E, Sundan A, Skjåk-Bræk G. The impact of chain length and flexibility in the interaction between sulfated alginates and HGF and FGF-2. Biomacromolecules 2015; 16(11):3417–3424.
23. Schmidt J, Lee MK, Ko E, Jeong JH, DiPietro LA, Kong H. Alginate Sulfates Mitigates Binding Kinetics of Proangiogenic Growth Factors with Receptors toward Revascularization. Mol Pharm 2016; 13(7):2148–2154.
24. Freeman I, Kedem A, Cohen S. The effect of sulfation of alginate hydrogels on the specific binding and controlled release of heparin-binding proteins. Biomaterials 2008;29(22):3260–3268.
25. Re'em T et al. Simultaneous regeneration of articular cartilage and subchondral bone induced by spatially presented TGF-beta and BMP-4 in a bilayer affinity binding system. Acta Biomater 2012;8(9): 3283–3293.
26. Freeman I, Cohen S. The influence of the sequential delivery of angiogenic factors from affinity-binding alginate scaffolds on vascularization. Biomaterials 2009;30(11):2122–2131.
27. Ruvinov E, Leor J, Cohen S. The effects of controlled HGF delivery from an affinity-binding alginate biomaterial on angiogenesis and blood perfusion in a hindlimb ischemia model. Biomaterials 2010; 31(16):4573–4582.

28. Ruvinov E, Leor J, Cohen S. The promotion of myocardial repair by the sequential delivery of IGF-1 and HGF from an injectable alginate biomaterial in a model of acute myocardial infarction. Biomaterials 2011;32(2):565–578.

29. Capulli A et al. Fibrous scaffolds for building hearts and heart parts. Adv Drug Deliv Rev 2016;96:83–102.

30. Peng S, Jin G, Li L, Li K, Srinivasan M, Ramakrishna S, Chen J. Multi-functional electrospun nanofibres for advances in tissue regeneration, energy conversion & storage, and water treatment. Chem Soc Rev 2016;45(5):1225–1241.

31. Akbari M, Tamayol A, Bagherifard S, Serex L, Mostafalu P, Faramarzi N, Mohammadi MH, Khademhosseini A. Textile Technologies and Tissue Engineering: A Path Toward Organ Weaving. Adv Healthc Mater 2016;5(7):751–766.

32. Tamayol A, Akbari M, Annabi N, Paul A, Khademhosseini A, Juncker D. Fiber-based tissue engineering: Progress, challenges, and opportunities. Biotechnol Adv 2013;31(5):669–687.

33. Semnani D, Naghashzargar E, Hadjianfar M, Dehghan Manshadi F, Mohammadi S, Karbasi S, Effaty F. Evaluation of PCL/chitosan electrospun nanofibers for liver tissue engineering. Int J Polym Mater Polym Biomater 2017;66(3):149–157.

34. Xin S, Li X, Wang Q, Huang R, Xu X, Lei Z, Deng H. Novel layer-by-layer structured nanofibrous mats coated by protein films for dermal regeneration. J Biomed Nanotechnol 2014;10(5):803–810.

35. Sadeghi D, Karbasi S, Razavi S, Mohammadi S, Shokrgozar MA, Bonakdar S. Electrospun poly (hydroxybutyrate)/chitosan blend fibrous scaffolds for cartilage tissue engineering. J Appl Polym Sci 2016;133(47):44171.

36. Najafabadi AH, Tamayol A, Annabi N, Ochoa M, Mostafalu P, Akbari M, Nikkhah M, Rahimi R, Dokmeci MR, Sonkusale S, Ziaie B, Khademhosseini A. Biodegradable nanofibrous polymeric substrates for generating elastic and flexible electronics. Adv Mater 2014;26(33):5823–5830.

37. Kharaziha M, Nikkhah M, Shin SR, Annabi N, Masoumi N, Gaharwar AK, Camci-Unal G, Khademhosseini A. PGS: Gelatin nanofibrous scaffolds with tunable mechanical and structural properties for engineering cardiac tissues. Biomaterials 2013;34(27):6355–6366.

38. Hasan A, Memic A, Annabi N, Hossain M, Paul A, Dokmeci MR, Dehghani F, Khademhosseini A. Electrospun scaffolds for tissue engineering of vascular grafts. Acta Biomater 2014;10(1):11–25.

39. Sridhar R, Lakshminarayanan R, Madhaiyan K, Amutha Barathi V, Lim KHC, Ramakrishna S. Electrosprayed nanoparticles and electrospun nanofibers based on natural materials: applications in tissue regeneration, drug delivery and pharmaceuticals. Chem Soc Rev 2015;44(3):790–814.

40. Nie H, He A, Zheng J, Xu S, Li J, Han CC. Effects of chain conformation and entanglement on the electrospinning of pure alginate. Biomacromolecules 2008;9(5):1362–1365.

41. Jeong SI, Krebs MD, Bonino CA, Khan SA, Alsberg E. Electrospun Alginate Nanofibers with Controlled Cell Adhesion for Tissue Engineeringa. Macromol Biosci 2010;10(8):934–943.

42. Bhattarai N, Li Z, Edmondson D, Zhang M. Alginate-based nanofibrous scaffolds: Structural, mechanical, and biological properties. Adv Mater 2006;18(11):1463–1467.

43. Linh NTB et al. Fabrication of polyvinyl alcohol/gelatin nanofiber composites and evaluation of their material properties. J Biomed Mater Res B Appl Biomater 2010;95((1):184–191.

44. Wang X, Ding B, Sun G, Wang M, Yu J. Electro-spinning/netting: a strategy for the fabrication of three-dimensional polymer nano-fiber/nets. Progress in Materials Science 2013;58(8):1173–1243.

45. Zhu Y, Wu C, Zhang Y, Zhao J. Study on the chain entanglement of polyvinyl alcohol fiber during the dry-jet wet spinning process. Fibers and Polymers 2015;16(2):345–353.

46. Sundarrajan S, Venkatesan A, Agarwal SR, Shaik Anwar Ahamed NN, Ramakrishna S. Fabrication of NiO/zirconium oxide nanofibers by electrospinning. Mater Sci Eng C 2014;45:369–373.

47. Lawrie G, Keen I, Drew B, Chandler-Temple A, Rintoul L, Fredericks P, Grøndahl L. Interactions between alginate and chitosan biopolymers characterized using FTIR and XPS. Biomacromolecules 2007;8(8):2533–2541.

48. Vatankhah E, Prabhakaran MP, Semnani D, Razavi S, Zamani M, Ramakrishna S. Phenotypic modulation of smooth muscle cells by chemical and mechanical cues of electrospun Tecophilic/gelatin nanofibers. ACS Appl Mater Interfaces 2014;6(6):4089–4101.

49. Safi S, Morshed M, Hosseini Ravandi SA, Ghiaci M. Study of electrospinning of sodium alginate, blended solutions of sodium alginate/poly (vinyl alcohol) and sodium alginate/poly (ethylene oxide). J Appl Polym Sci 2007;104(5):3245–3255.

50. Coleman MM, Painter PC. Hydrogen bonded polymer blends. Prog Polym Sci 1995;20(1):1–59.

51. Boontheekul T, Kong H-J, Mooney DJ. Controlling alginate gel degradation utilizing partial oxidation and bimodal molecular weight distribution. Biomaterials 2005;26(15):2455–2465.

52. Fan L, Jiang L, Xu Y, Zhou Y, Shen Y, Xie W, Long Z, Zhou J. Synthesis and anticoagulant activity of sodium alginate sulfates. Carbohydr Polym 2011;83(4):1797–1803.

53. Ronghua H, Yumin D, Jianhong Y. Preparation and in vitro anticoagulant activities of alginate sulfate and its quaterized derivatives. Carbohydr Polym 2003;52(1):19–24.

54. Arlov Ø, Aachmann FL, Sundan A, Espevik T, Skjåk-Bræk G. Heparin-Like Properties of Sulfated Alginates with Defined Sequences and Sulfation Degrees. Biomacromolecules 2014;15(7):2744–2750.

55. Destaye AG, Lin C-K, Lee C-K. Glutaraldehyde vapor cross-linked nanofibrous PVA mat with in situ formed silver nanoparticles. ACS Appl Mater Interfaces 2013;5(11):4745–4752.

56. Canbolat MF, Gera N, Tang C, Monian B, Rao BM, Pourdeyhimi B, Khan SA. Preservation of cell viability and protein conformation on immobilization within nanofibers via electrospinning functionalized yeast. ACS Appl Mater Interfaces 2013;5(19):9349–9354.

57. Van Vlierberghe S, Dubruel P, Schacht E. Biopolymer-based hydrogels as scaffolds for tissue engineering applications: a review. Biomacromolecules 2011;12(5):1387–1408.

58. Bolto B, Tran T, Hoang M, Xie Z. Crosslinked poly (vinyl alcohol) membranes. Prog Polym Sci 2009;34(9):969–981.

59. Pirzada T, Arvidson SA, Saquing CD, Shah SS, Khan SA. Hybrid silica–PVA nanofibers via sol–gel electrospinning. Langmuir 2012;28(13):5834–5844.

60. Slaughter BV, Khurshid SS, Fisher OZ, Khademhosseini A, Peppas NA. Hydrogels in regenerative medicine. Adv Mater 2009;21(32–33):3307–3329.

61. Lee JS, Choi KH, Ghim HD, Kim SS, Chun DH, Kim HY, Lyoo WS. Role of molecular weight of atactic poly (vinyl alcohol)(PVA) in the structure and properties of PVA nanofabric prepared by electrospinning. J Appl Polym Sci 2004;93(4):1638–1646.

62. Lee YJ, Shin DS, Kwon OW, Park WH, Choi HG, Lee YR, Han SS, Noh SK, Lyoo WS. Preparation of atactic poly (vinyl alcohol)/sodium alginate blend nanowebs by electrospinning. J Appl Polym Sci 2007;106(2):1337–1342.

63. Hassan CM, Peppas NA. Structure and applications of poly (vinyl alcohol) hydrogels produced by conventional crosslinking or by freezing/thawing methods, in Biopolymers· PVA Hydrogels, Anionic Polymerisation Nanocomposites. Berlin, Heidelberg: Springer; 2000. p 37–65.

64. Liang D, Hsiao BS, Chu B. Functional electrospun nanofibrous scaffolds for biomedical applications. Adv Drug Deliv Rev 2007;59(14):1392–1412.

65. Zhang X, Reagan MR, Kaplan DL. Electrospun silk biomaterial scaffolds for regenerative medicine. Adv Drug Deliv Rev 2009;61(12):988–1006.

66. Ruvinov E, Cohen S. Alginate biomaterial for the treatment of myocardial infarction: progress, translational strategies, and clinical outlook: from ocean algae to patient bedside. Adv Drug Deliv Rev 2016;96:54–76.

67. Silva EA, Mooney DJ. Effects of VEGF temporal and spatial presentation on angiogenesis. Biomaterials 2010;31(6):1235–1241.

68. Bonakdar S, Emami SH, Shokrgozar MA, Farhadi A, Ahmadi SAH, Amanzadeh A. Preparation and characterization of polyvinyl alcohol hydrogels crosslinked by biodegradable polyurethane for tissue engineering of cartilage. Mater Sci Eng C 2010;30(4):636–643.

69. Vunjak-Novakovic, G. and R.I. Freshney, Culture of cells for tissue engineering. Vol. 7. Hoboken, New Jersey: John Wiley & Sons, 2006.

70. Hajiali H, Heredia-Guerrero JA, Liakos I, Athanassiou A, Mele E. Alginate nanofibrous mats with adjustable degradation rate for regenerative medicine. Biomacromolecules 2015;16(3): 936–943.

71. Vacanti NM, Cheng H, Hill PS, Guerreiro JDT, Dang TT, Ma M, Watson S, Hwang NS, Langer R, Anderson DG. Localized delivery of dexamethasone from electrospun fibers reduces the foreign body response. Biomacromolecules 2012;13(10):3031–3038.

72. Chaubaroux C, Vrana E, Debry C, Schaaf P, Senger B, Voegel JC, Haikel Y, Ringwald C, Hemmerlé J, Lavalle P, Boulmedais F. Collagen-based fibrillar multilayer films cross-linked by a natural agent. Biomacromolecules 2012;13(7):2128–2135.